

# Effective temperatures, rotational velocities, microturbulent velocities and abundances in the atmospheres of the Sun, HD1835 and HD10700

Ya. V. Pavlenko<sup>1,2\*</sup>, J.S. Jenkins<sup>2,3</sup>, H.R.A. Jones<sup>2</sup>, O.M. Ivanyuk<sup>1</sup>, D.J. Pinfield<sup>2</sup>

<sup>1</sup>*Main Astronomical Observatory, Academy of Sciences of Ukraine, Golosiiv Woods, Kyiv-127, 03680 Ukraine*

<sup>2</sup>*Centre for Astrophysics Research, University of Hertfordshire, College Lane, Hatfield, Hertfordshire AL10 9AB, UK*

<sup>3</sup>*Departamento de Astronomía, Universidad de Chile, Camino del Observatorio 1515, Las Condes, Santiago, Chile*

## ABSTRACT

We describe our procedure to determine effective temperatures, rotational velocities, microturbulent velocities, and chemical abundances in the atmospheres of Sun-like stars. We use independent determinations of iron abundances using the fits to the observed Fe I and Fe II atomic absorption lines. We choose the best solution from the fits to these spectral features for the model atmosphere that provides the best confidence in the determined  $\log N(\text{Fe})$ ,  $V_t$ , and  $v \sin i$ . Computations were done in the framework of LTE. Blending effects were accounted for explicitly. First, we compute the abundance of iron for a set of adopted microturbulent velocities. In some cases, a few points of  $\log N(\text{Fe I}) = \log N(\text{Fe II})$  can be found. To determine the most self-consistent effective temperature and microturbulent velocity in any star's atmosphere, we used an additional constraint where we minimise the dependence of the derived abundances of Fe I and Fe II on the excitation potential of the corresponding lines. Using this procedure we analyse the spectra of the Sun and two well known solar type stars, HD1835 and HD10700 to determine their abundances, microturbulent velocity and rotational velocity. Our approach allows us to determine self-consistent values for the effective temperatures, abundances,  $V_t$  and  $v \sin i$ . For the Sun we obtain the best agreement for a model atmosphere of  $T_{\text{eff}} / \log g / [\text{Fe}/\text{H}] = 5777/4.44/0.0$ , iron abundances and microturbulent velocities of  $\log N(\text{Fe}) = 4.44$ ,  $V_t = 0.75$  km/s, for the Fe I lines, and  $\log N(\text{Fe}) = -4.47$ ,  $V_t = 1.5$  km/s for the Fe II lines. Furthermore, abundances of other elements obtained from the fits of their absorption features agree well enough ( $\pm 0.1$  dex) with the known values for the Sun. We determined a rotational velocity of  $v \sin i = 1.6 \pm 0.3$  km/s for the spectrum of the Sun as a star. For HD1835 the self-consistent solution for Fe I and Fe II lines  $\log N(\text{Fe}) = +0.2$  was obtained with a model atmosphere of  $5807/4.47/+0.2$  and microturbulent velocity  $V_t = 0.75$  km/s, and leads to  $v \sin i = 7.2 \pm 0.5$  km/s. For HD10700 the self-consistent solution  $\log N(\text{Fe}) = -4.93$  was obtained using a model atmosphere of  $5383/4.59/-0.6$  and microturbulent velocity  $V_t = 0.5$  km/s. The Fe I and Fe II lines give rise to a  $v \sin i = 2.4 \pm 0.4$  km/s. Using the  $T_{\text{eff}}$  found from the ionisation equilibrium parameters for all three stars, we found abundances of a number of other elements: Ti, Ni, Ca, Si, Cr. We show that uncertainties in the adopted values of  $T_{\text{eff}}$  of 100 K and  $V_t$  of 0.5 km/s change the abundances of elements up to 0.1 and 0.2 dex respectively. Galactic abundances variations can generally be larger than this measurement precision and therefore we can study abundance variations throughout the Galaxy.

**Key words:** stars: molecular spectra stars: fundamental parameters – stars: late-type – stars: evolution –

**Table 1.** Temperatures, gravities and abundances used in studies of HD1835.

$T_{\text{eff}}$	log $g$	[Fe/H]	Comp. Star	Reference
5857	4.47	+0.23	Sun	This Paper
5764	4.40	+0.21	Sun	Jenkins et al. (2008)
5767	4.45	+0.16	Sun	Soubiran et al. (2008)
5857	4.47	+0.22	Sun	Valenti & Fisher (2005)
5673	4.22	-0.01	Sun	Pasquini et al. (1994)
5793	4.50	+0.20	Sun	Boesgaard & Friel (1990)
5793	4.60	+0.24	Sun	Abia et al. (1988)
5793	-	+0.16	Sun	Boesgaard & Budge (1988)
5860	4.40	+0.28	Sun	Rebolo et al. (1986)
5793	4.50	+0.19	Sun	Cayrel de Strobel et al. (1985)
5860	4.40	-0.09	Sun	Cayrel de Strobel et al. (1981)

## 1 INTRODUCTION

In the past the majority of research conducted on solar-type stars was focused on accurately constraining their physical parameters, such as effective temperature, bolometric magnitude, radius, metallicity and color indices using a variety of different photometric and spectroscopic techniques (e.g. Glushneva et al. 2002). However, with the advance of technology, high resolution echelle spectrographs and more observing time, the field is pushing to even higher precision measurements for a larger database of atomic and molecular species in stellar atmospheres (e.g. Valenti & Fischer 2005; Neves et al. 2009; Mashonkina et al. 2011) and more precise physical parameters from the latest evolutionary models (Lopez-Santiago et al. 2010; Ghezzi et al. 2010; Takeda et al. 2010; Tabernero et al. 2011). One of the main reasons for the growing interest into solar-type stars is that the metal content of planet-hosting stars is an important ingredient that seems to affect the formation and evolution of planetary systems (see Israelian 2010; Santos et al. 2011; Sousa et al. 2012, and reference therein).

Valenti & Fischer have published an extended uniform catalog of stellar properties for 1040 nearby F, G, and K stars that were observed by the Keck, Lick, and AAT planet search programs. Accurate stellar abundances from spectral synthesis fitting requires the determination of reliable physical parameters, namely the effective temperature, surface gravity, microturbulent velocity, rotational velocity and atomic abundances (see Jenkins et al. 2008; Jenkins et al. 2009a). Studying stars with spectral types similar to the Sun but with other physical differences can help to test new analysis techniques.

HD1835 is a variable and magnetically active G3V star (see Jenkins et al. 2006, Martínez-Arnáiz, 2010) In Table 1 we show the iron abundances studied by different authors for HD1835. When we look at past studies there is a fairly large spread in metallicities for this star, however, in recent times there is more convergence towards the star having super-solar metallicity. Only two studies found this star to have sub-solar metallicity, the last back in 1994.

HD10700 is a high proper-motion dwarf star, studied by many authors. Simbad lists 756 references as of February 2012, ranging from chromospheric activity studies (Jenkins et al. 2006, Martínez-Arnáiz et al. 2010) through to stel-

**Table 2.** Temperatures, gravities and abundances used in studies of HD10700.

$T_{\text{eff}}$	log $g$	[Fe/H]	Comp. Star	Reference
5383	4.59	-0.55	Sun	This Paper
5377	4.53	-0.49	Sun	Mashonkina et al. (2011)
5522	4.50	-0.37	Sun	Jenkins et al. (2008)
5344	4.45	-0.52	Sun	Soubiran et al. (2008)
5310	4.44	-0.52	-	Sousa et al. (2008)
5264	4.36	-0.50	Sun	Cenarro et al. (2007)
5283	4.59	-0.52	Sun	Valenti & Fischer (2005)
5320	4.30	-0.50	Sun	Castro et al. (1999)
5330	4.30	-0.59	Sun	Tomkin et al. (1999)
5500	4.32	-0.38	Sun	Mallik et al. (1998)
5250	4.65	-0.46	Sun	Arribas et al. (1989)
5143	3.60	-0.60	Sun	Barbuj et al. (1989)
5305	4.32	-0.66	Sun	Gratton (1989)
5250	4.50	-0.58	Sun	Abia et al. (1988)
4990	4.50	-0.56	Sun	Francois (1986)
5305	4.33	-0.49	Sun	Steenbock (1983)
5362	4.59	-0.34	Sun	Hearnshaw (1974)
5538	-	-0.13	Sun	Herbig (1965)
5196	-	-0.39	Sun	Pagel et al. (1964)
5305	-	-0.39	Sun	Pagel (1963)

lar oscillation studies (Teixeira et al. 2009). In Table 2 we show the iron abundances studied by different authors for HD10700.

The overall goal of this paper is to outline our new procedure to measure precise and accurate iron abundances, microturbulent velocities and rotational velocities for solar-type stars through analysis of high resolution stellar spectra of the Sun, HD1835 and HD10700.

## 2 PROCEDURE

### 2.1 Observed data

The adopted parameters for our stars are listed in Table 3. The spectra and all calibration data were observed using the Fibre-fed Extended Range Optical Spectrograph (FEROS) mounted on the MPG/ESO - 2.2m telescope on the La Silla site in Chile. The exposure times were long enough to ensure that the spectra were observed with S/N ratios of well over 150 in the continuum around the iron lines at 6100 Å at the operating resolution of FEROS ( $R \sim 48'000$ ). All calibration files needed for the reduction of the stellar spectra (flat-fields, bias and arc frames) were obtained at the beginning and end of each nights observing, following the standard ESO calibration plan. The reduction of all the spectra followed the standard reduction techniques described by Jenkins et al. (2008).

The observed spectrum of the Sun (Kurucz et al. 1984) is used as the reference star. The resolution of the solar spectrum is much higher, ( $R = 100'000$ ), however profiles of observed lines in the solar spectrum are broadened by macroturbulence. We adopt a gaussian for the macroturbulence profile with a FWHM = 0.1Å at 6000Å. This corresponds to  $V_{\text{macro}} = 2.2 \text{ km s}^{-1}$  which agrees well with the reference value (Gurtovenko & Sheminova 1986).

**Table 3.** Parameters of stars of our interest

Star	$T_{\text{eff}}$ (VF05)	$\log g$ (VF05)	[Fe/H] (VF05)	$V_r$ (km/s)	$v \sin i$ (km/s)
the Sun	5777	4.44	0		1.7
HD1835	5857.0±22	4.47	+0.22	-2.7±1.8 (Jenkins et al. 2011)	6 (VF05), 8 (Jenkins et al. 2008)
HD10700	5283±22	4.59	-0.52	-16.9±1.6 (Jenkins et al. 2011)	2 (VF05)

## 2.2 Model atmospheres

HD1835 and HD10700 are stars which are similar to the Sun, validating the Sun as our reference star. For each star we computed plane-parallel model atmospheres in LTE, with no energy divergence, using the SAM12 program (Pavlenko 2003), which is a modification of ATLAS12 (Kurucz 1999). In this study as “the zeroth approach” we adopt values given by Valenti & Fischer (2005) for both stars HD1835 and HD10700, i.e..  $T_{\text{eff}} / \log g / [\text{Fe}/\text{H}] = 5857/4.47/+0.22$  and  $5383/4.75/-0.36$ , respectively, for faster convergence of the code. For the Sun we used a model atmosphere of  $5777/4.44/0.00$ . All models were recomputed with the new abundances found by ourselves. Chemical equilibrium is computed for molecular species assuming LTE and we use the opacity sampling approach from Sneden (1976) to account for absorption of atoms, ions and molecules (see more details in Pavlenko 2003). The 1-D convective mixing length theory, modified by Kurucz (1999) in ATLAS12, was used to account for convection. The computed model atmospheres are available on the web<sup>1</sup>.

## 2.3 Synthetic spectra

Synthetic spectra are calculated with the WITA6 program (Pavlenko 1997), using the same approximations and opacities as SAM12. To compute the synthetic spectra we use line lists taken from VALD2 (Kupka et al. 1999). The shape of each atomic line is determined using a Voigt function and all damping constants are taken from line databases, or computed using Unsold’s approach (Unsold 1954). A wavelength step of  $\Delta\lambda = 0.025 \text{ \AA}$  is employed in the synthetic spectra computations to match our observed FEROS spectrum. It is worth noting that different atomic species provide different contributions to the formation of the spectrum of solar-like stars. In particular, iron lines dominate the solar spectrum.

## 2.4 Best fit parameters selection

In our work we used two spectroscopic datasets to carry out the abundance analysis. The first one consists of the spectroscopic data taken from the VALD (Kupka et al. 1999). For any absorption line we identify the atom, molecule or ion, its central wavelength,  $\lambda_o$ , the oscillator strength of the transition  $gf$ , the excitation potential of the lower level  $E''$  of the corresponding transition and the damping constants  $C_2, C_4, C_6$ . The second one contains the list of pre-selected spectral regions ( $N_L$ ) governed by absorption of the atom and/or ion of interest.

### 2.4.1 Pre-selection of spectral features in the solar spectrum

We used the Sun as a template star to verify our procedure. Indeed, the solar abundances were determined by many authors using different procedures and the results do not differ very little.

The first step of our selection procedure was to compute a spectrum of the Sun taking into account only lines of elements of interest. A comparison with the observed spectrum provides a list of spectral features in which absorption of our element dominates. Blending by other lines was accounted for directly where the contribution of other lines can be estimated in a simple way from the analysis of the ratio  $r(\text{Fe})/r(\text{Sun})$ , where  $r(\text{Fe})$  and  $r(\text{Sun})$  are residual fluxes from the continuum normalisation in our theoretical spectrum of iron lines and the observed spectrum of the Sun. Then, from the analysis of the shape of the  $r(\text{Fe})/r(\text{Sun})$  ratio we determine the central wavelengths of every feature and spectral region in which we compare the theoretical and observed spectra to determine the iron abundance. The spectral range of comparison was chosen to be approximately between  $-0.1\text{\AA}$  and  $+0.1\text{\AA}$  from the blue and red edge of the corresponding spectral feature, a method shown to be effective in Jenkins et al. (2008). We do note that the synthetic spectra were computed across a broader spectral region of approximately  $\pm 5 \text{ \AA}$ .

From a comparison of the observed and computed spectra we obtained a list of strong features governed by the absorption of a given element. Strong features were selected to reduce the possible effects of noise. As a limit for our strong lines we choose the value  $r(\text{Fe}) = 0.8$ .

### 2.4.2 Fits to pre-selected spectral features

For each preselected spectral region that contains an absorption line we are interested in, we carry out the fit to the observed spectrum. The synthetic spectra that are computed across the selected spectral region are convolved with profiles that match the instrumental broadening and that take into account rotational broadening. For instrumental broadening we adopt a Gaussian profile and the rotational broadening was treated following the scheme by Gray (1976). The instrumental broadening takes care of the spectrograph resolution, and  $v \sin i$  is a parameter used to get the best fit to the observed profiles of any feature in our spectrum.

For every feature we find the minimisation parameter:

$$S_1 = \sum (1 - r_\nu^s/r_\nu^o)^2 / N_o$$

here  $N_o$  is the number of points in the observed spectrum across the pre-selected spectral region,  $r_\nu^o$  and  $r_\nu^s$  are residual fluxes in the observed and computed spectra, respec-

<sup>1</sup> ftp://ftp.mao.kiev.ua/pub/users/yp/MA2010

tively. Formally a minimum  $S_l$  determines our solution, i.e. the abundance of an element governed by the associated absorbing feature on the adopted set of abundances  $X_i = \log(N(X_i)), i = 1, \dots, N_a$ , where  $N_a$  is the dimensionality of the abundance grid.

Our measurements are affected by some errors of a differing nature: uncertainties in  $gf$ , blending, presence of noise in the observed spectrum, etc. Every fitted spectral feature provides one abundance  $X_l$  on  $\min S_l, l = 1, N_L$  we compute mean abundance

$$X_o = (\sum X_l)/L$$

and a formal standard error  $\sigma_o$

$$\sigma_o = \sqrt{\sum (X_l - X_o)^2 / (N_l * (N_l - 1))}$$

where  $N_l$  is the total number of the fitted spectral lines.

It is worth noting that sometimes not all pre-selected features provide a minimum  $S$  on our grid of abundances, therefore  $N_l \leq N_L$ . In other words, if the minimum of  $S$  cannot be found in the adopted abundance range, or any absorption feature is too weak in the observed spectrum, the line was excluded from the following consideration.

Additionally, we compute the abundance of elements averaged over  $1\sigma$ , i.e. we averaged all abundances across  $X_o + 1\sigma_o$ :

$$X_s = \sum (X_l/\sigma_l) / \sum (1/\sigma_l)$$

In this paper we adopt  $N_a = 30$  with a step of 0.05,  $N_v = 6$  with a step of 0.5 km/s and  $N_r = 11$  with a step of 0.4 - 0.5 km/s.

In some details our procedure is similar to that used by Jones et al. (2002) and Pavlenko & Jones (2002), but in this case we individually fit the synthetic spectra to the pre-selected features in the observed spectrum.

Our procedure allows us to obtain the iron abundances from the fits to Fe I and Fe II independently. The Fe I/Fe II =  $\log N(\text{Fe I}) - \log N(\text{Fe II})$ , where  $N(\text{Fe I})$  and  $N(\text{Fe II})$  are respectively the iron abundance determined from the fits to Fe I and Fe II lines, is used to verify the  $\log g$  of the model atmospheres used in the fits.

It is worth noting a few important points:

- since we deal with blending by absorption lines of other elements, which allows us to include strong blended features in the observed spectrum.
- rotational velocity ( $v \sin i$ ) is determined for every point ( $\log N(\text{Fe}), V_t$ ) of our synthetic spectral grid for every spectral line.

## 2.5 General algorithm of solution

### 2.5.1 Dependence of abundance of iron vs. excitation potential of absorption lines

In our analysis we use a set of lines of different excitation potentials of the lower level of the corresponding radiative transition  $E''$ . In the first approach their response on temperature in the line-forming region of the stellar atmosphere can be described by  $\exp(-E''/kT)$ , where the labels have

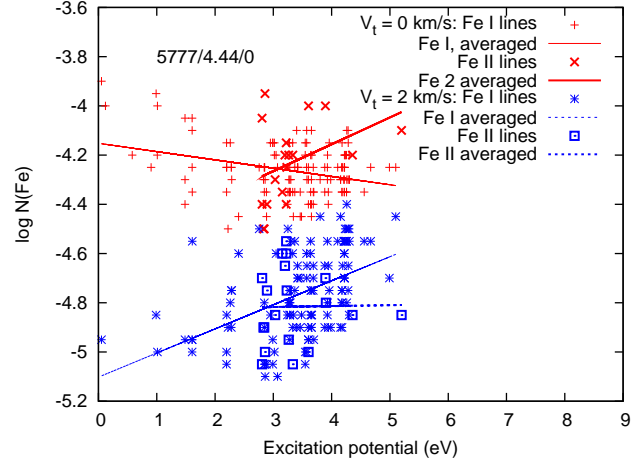


**Figure 1.** Dependence of the iron abundance determined from the fits to the observed Fe I and Fe II features in the observed spectrum of the Sun vs. excitation potential computed for a model atmosphere with parameters 5777/4.44/0.

the conventional meaning. Lines of different  $E''$  show different response to  $T$  (and respectively, on  $T_{\text{eff}}$ ). In our case we work with blends in the stellar spectra too. They are treated explicitly. If a few lines of the given element form the feature then we use the “effective” excitation potential

$$E'' = -\ln(\sum(g_i * \exp(-E_i/kT)) / \sum(g_i)) * kT$$

here values and labels have the conventional meaning,  $i = 1, \dots, N$ . Here  $N$  is the total number of lines of the given element that formed the feature.

Ideally, for the properly determined  $T_{\text{eff}}$  we should not obtain any dependence of  $\log N(\text{Fe})$  on  $E''$  for absorption lines of both Fe I and Fe II. In other words the absence of dependence of  $\log N(\text{Fe}) = f(E'')$  we consider as a sufficient condition for the determination of microturbulent velocity and abundance. It is worth noting that a similar approach was used by other authors in the past (see fig.8 in Mashonkina et al 2011).

In Fig. 1 we plot the dependence of Fe I and Fe II abundances in the spectrum of the Sun versus their excitation potentials. These computations were carried out for a model atmosphere of 5777/4.44 and microturbulent velocities of  $V_t = 0$  km/s and 2 km/s. The results of the approximation of the dependence of  $\log N(\text{Fe}) = f(E'')$  is highlighted by the straight line fits to the data in the figure.

Even visual inspection of Fig. 1 provides a good estimation of microturbulence velocity in the solar atmosphere  $0 < V_t < 2$  km/s. A more complete set of the approximations obtained for  $V_t = 0, 0.5, 1, 1.5, 2, 2.5$  km/s will be shown in section 3 for our star of interest.

### 2.5.2 The self-consistent solution

We pay special attention to the ionisation equilibrium Fe I/Fe II. Lines of these ions are abundant in the spectra of solar-like stars. Furthermore, the spectroscopic data for Fe I and Fe II lines are more accurate and complete in comparison with other ions.

To determine the realistic parameters of our stars we developed and used the following custom algorithm:

1) Using the fits to the profiles of Fe I and Fe II lines separately, we compute dependences of  $\log N(\text{Fe}) = f(V_t)$  for the model atmosphere with adopted  $T_{\text{eff}}$  on a fixed grid of microturbulence velocities. In general  $\log N(\text{Fe I}) = \log N(\text{Fe II})$  is a pre-requisite to find the proper  $T_{\text{eff}}$ .

2) In some cases we obtain a few solutions  $\log N(\text{Fe I}) = \log N(\text{Fe II})$  for different  $T_{\text{eff}}$  and  $V_t$ , and  $v \sin i$ . To select the best solution we test if there is any dependence of derived abundances on excitation potential of lower level of the corresponding spectral features, as described in section 2.4.2.

3) After the determination of  $\log N(\text{Fe})$ ,  $T_{\text{eff}}$ ,  $V_t$  we determined the abundances of other elements.

4) If we obtain large differences in abundances in comparison with the results of the previous iteration then we recompute the model atmosphere and repeat all these procedures.

It is worth noting that in comparison with the former papers we reduced the number of free parameters. Namely, we determined  $\log N(\text{Fe})$ ,  $V_t$  and  $v \sin i$  from the best fit to the observed spectrum. Then, we used an averaging procedure across the  $1\sigma$  error parameter space to obtain a statistically significant result. Finally, the best solution was found from the best agreement of all three parameters on the grid of parameters. Furthermore, the metallicity of the model atmosphere agrees with the fitting results, i.e.. we found our final solution in a few successive approximations taking into account the variability of the abundances and other parameters in only a few iterations.

### 3 RESULTS

#### 3.1 Formal test of the procedure: abundances, $V_t$ , and $v \sin i$ for the Sun

To test our procedure we employed a few model atmospheres with parameters 5777/4.44, 5777/4.50, 5527/4.50 and 6027/4.50. We then determined  $\log(\text{Fe})$  for the adopted grid of microturbulent velocities  $V_t = 0, 0.5, 1, 1.5, 2, 2.5$  km/s using the fits to Fe I and Fe II lines in the observed solar spectrum. Error bars were computed following the standard procedure described in section 2.4.2.

Results of the iron determinations for three model atmospheres are shown in Fig. 2. As was expected, only model atmospheres with  $T_{\text{eff}} = 5777$  K provide similar values of iron abundances obtained from the fits of Fe I and Fe II lines. Model atmospheres of lower  $T_{\text{eff}}$  provide overestimated abundances of Fe II ions in the atmosphere of the Sun and underestimate the abundances of Fe I, respectively, and vice versa, model atmospheres of higher  $T_{\text{eff}}$ , underestimate abundances of Fe II and overestimate Fe I.

It is worth briefly noting two points:

- Visual inspection of the plots similar to that shown in Fig 2 can be used to determine the proper  $T_{\text{eff}}$ .
- We see good agreement in iron abundances obtained from the fits of Fe I and Fe II lines across the wide range of microturbulent velocities for the model atmospheres 5777/4.44 and 5777/4.5.

To solve the last problem we investigated the obtained abundances versus excitation potential of the main absorbing lines. We approximate the obtained dependence of computed abundances versus  $E''$  by a linear function using least-squares fitting. The dependence  $\log N(\text{Fe})$  vs..  $E''$  computed for a model atmosphere of the Sun of 5777/4.44/0.0 and different microturbulent velocities is shown in the lower panel of Fig. 2. Results of fits to Fe I lines show the absence of the  $\log N(\text{Fe})$  vs.  $E''$  for  $V_t = 0.75$  km/s and  $\log N(\text{Fe}) = -4.40$ . It is worth noting that Sheminova & Gadun (2010) analysed the Sun at high resolution ( $R=200000$ ) and found  $V_t = 0.8 \pm 0.2$  km/s. Nevertheless, our value of iron abundance corresponds well enough with Grevesse and Anders (1979)  $\log N(\text{Fe}) = -4.37$  and Gurtovenko and Kostik (1989)  $\log N(\text{Fe}) = -4.40$ . However, our fits to Fe II lines provide a little lower abundance  $\log N(\text{Fe}) = -4.6$ . The differences of iron obtained from the fits to Fe I and Fe II lines are discussed in many papers (see the most recent paper Mashonkina et al. 2011 and discussion therein). On the other hand, our sample of Fe I lines is larger, therefore the results obtained from the fits to the the neutral ion lines in the observed spectrum are more robust.

Using the derived estimations of  $T_{\text{eff}}$ ,  $\log g$ , and  $V_t$  we obtained abundances of other elements using the aforementioned scheme. The comparison of our results with known abundances for the Sun is presented in Table 7. For most abundances where we found satisfactory agreement, the residuals do not exceed 0.1 dex. However, we found a difference of 0.16 dex against the Cr I abundance measured by Grevesse and Anders (1989). On the other hand our value agrees well with the Gurtovenko & Kostik value  $\log N(\text{Cr}) = -8.07$ . Therefore, we estimate our accuracy of abundance determination as  $< 0.1$  dex. This level of precision provides us with a good opportunity to investigate absolute differences in the abundances of stars like the Sun.

To investigate the dependence of abundances on the adopted microturbulent velocity we repeat our abundance determination procedure for the case of  $V_t = 1.25$  km/s (see Table 4). For all elements we obtained similar results, i.e. difference in the adopted microturbulent velocity of 0.5 km/s provide changes in the obtained abundances by a factor of 0.2 dex.

In Table 4 we show the rotational velocity of the Sun determined from the fits of our features to the observed spectrum of the Sun as a star (Kurucz et al. 1984). For the solar spectrum we adopt an effective resolution  $R = 70'000$ , the formal resolution limited by the presence of macroturbulent velocity  $V_{\text{ma}} = 1 - 2.6$  km/s (Gurtovenko & Sheminova 1986, Sheminova & Gadun 2010). Our determined  $v \sin i = 1.6 \pm 0.3$  agrees well with the known rotational velocity of the Sun  $v \sin i \sim 1.85 \pm 0.1$  km/s (see Bruning 1984), and corresponds well with  $v \sin i = 1.63$  km/s obtained by Valenti & Fisher (2005).

One may expect that the determined rotational velocity for the Sun depends on the adopted resolution. Indeed, even a slightly lower resolution of  $R = 60'000$  will overestimate the contribution from macroturbulence into the total broadening and underestimate the  $v \sin i = 1.2 \pm 0.3$  km/s.

However, it does not affect the results of abundance determinations because the observed spectra are broadened by the combined profile formed by rotation + macroturbulence

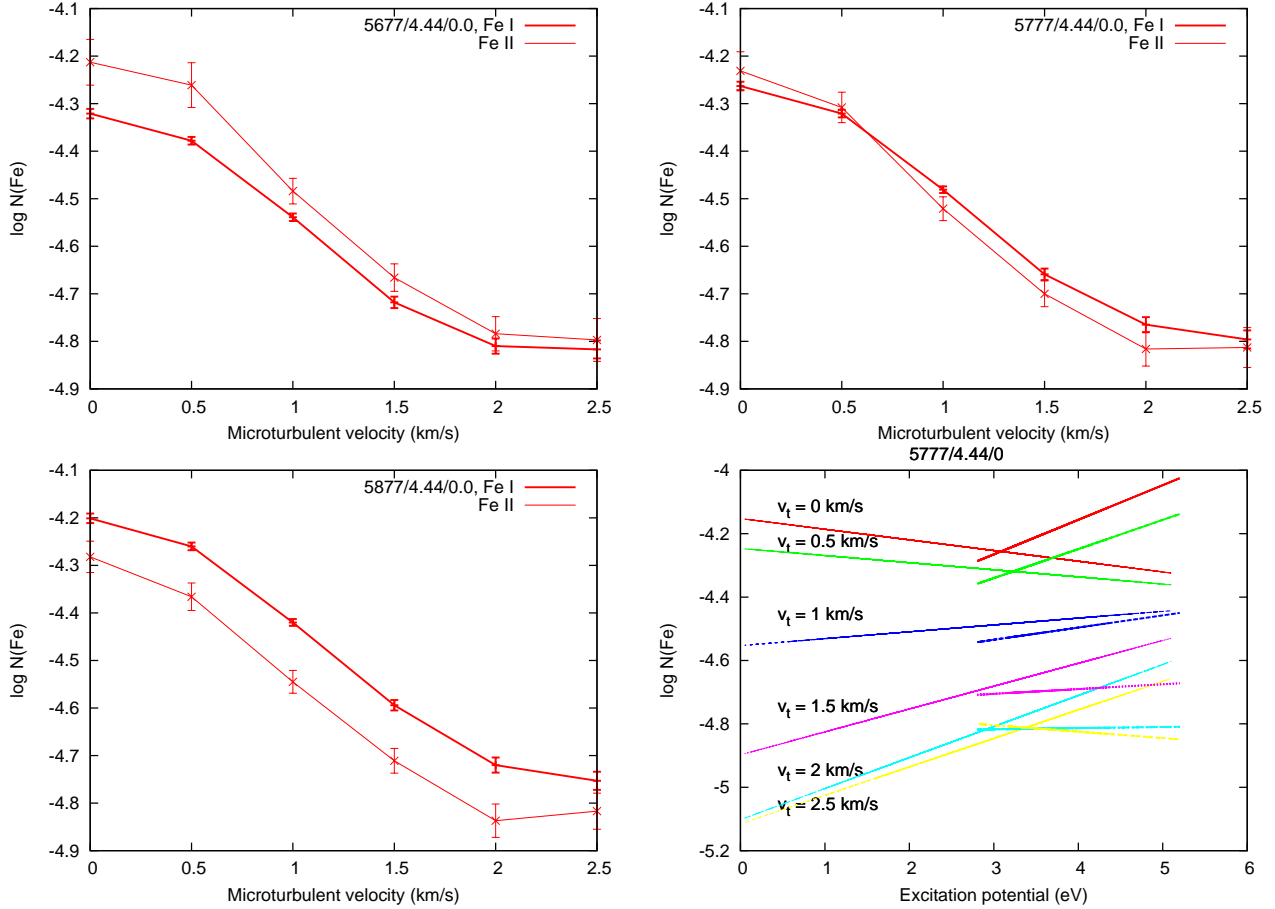


**Figure 2.** Abundances of iron determined from the fits to the observed Fe I and Fe II features in the observed spectrum of the Sun. Model atmospheres are 5677/4.44, 5777/4.44, and 5877/4.44 for the panels at the top left, top right, and lower left, respectively. The lower right panel shows the dependence of  $\log N(\text{Fe})$  vs.  $E''$  of Fe I and Fe II lines shown by thin and thick lines, respectively, used to computed the corresponding abundances for the model atmosphere of 5777/4.44.

**Table 4.** Abundances in the atmosphere of the Sun as a star

	$V_t = 0.75 \text{ km/s}$			$V_t = 1.25 \text{ km/s}$		
	Mean $X_o$	Averaged $X_s$	$v \sin i$	Mean $X_o$	Averaged $X_s$	$v \sin i$
Ca I	$-5.592 \pm 0.020$	$-5.609 \pm 0.114$	$1.300 \pm 0.392$	$-5.767 \pm 0.019$	$-5.777 \pm 0.105$	$1.133 \pm 0.342$
Cr I	$-6.307 \pm 0.021$	$-6.440 \pm 0.143$	$1.758 \pm 0.265$	$-6.473 \pm 0.018$	$-6.391 \pm 0.136$	$1.740 \pm 0.262$
Fe I	$-4.395 \pm 0.007$	$-4.394 \pm 0.005$	$1.644 \pm 0.144$	$-4.566 \pm 0.009$	$-4.514 \pm 0.004$	$1.598 \pm 0.140$
Fe II	$-4.418 \pm 0.023$	$-4.498 \pm 0.112$	$1.805 \pm 0.426$	$-4.603 \pm 0.026$	$-4.744 \pm 0.166$	$1.616 \pm 0.381$
Ni I	$-5.745 \pm 0.013$	$-5.621 \pm 0.054$	$1.743 \pm 0.247$	$-5.880 \pm 0.016$	$-5.787 \pm 0.043$	$1.555 \pm 0.220$
Ti I	$-7.027 \pm 0.019$	$-7.022 \pm 0.078$	$1.652 \pm 0.312$	$-7.237 \pm 0.020$	$-7.365 \pm 0.119$	$1.541 \pm 0.291$
Ti II	$-6.847 \pm 0.037$	$-6.602 \pm 0.176$	$1.944 \pm 0.381$	$-7.097 \pm 0.038$	$-6.863 \pm 0.136$	$1.841 \pm 0.361$

+ instrumental broadening, where the broadening shape is dominated by the instrumental profile.

### 3.2 HD1835

For HD1835 we obtained good agreement between abundances obtained from fitting the Fe I and Fe II lines over a wide range of  $V_t$  for model atmospheres of  $T_{\text{eff}}$  5807 and 5857 K. However, the additional proof of the dependence of

the obtained abundances on  $V_t$ , shown at the bottom right panel of Fig. 3, gives better results of  $\log N(\text{Fe}) = -4.18$  for the 5807/4.47/+0.2 model atmosphere and  $V_t = 0.75 \text{ km/s}$ . The abundances of other elements determined with these parameters are given in the Table 5.

For HD1835 we investigated the dependence of our abundance determination on  $T_{\text{eff}}$ . Differences of 100K in the adopted effective temperature changes the determined abundances by only 0.1 dex. As for the Sun, the formal ac-

**Table 5.** Abundances in the atmosphere of HD1835

	5807/4.47/+0.2, $V_t = 0.75$ km/s			5857/4.47/+0.2, $V_t = 0.75$ km/s		
	Mean log [X/H]	log [X/H] averaged	$v \sin i$	Mean log [X/H]	log [X/H] averaged	$v \sin i$
Ca I	$-5.262 \pm 0.036$	$-5.322 \pm 0.213$	$7.000 \pm 2.111$	$-5.229 \pm 0.040$	$-5.282 \pm 0.121$	$7.042 \pm 2.123$
Cr I	$-6.016 \pm 0.034$	$-6.017 \pm 0.121$	$7.560 \pm 1.181$	$-6.000 \pm 0.032$	$-6.203 \pm 0.083$	$7.500 \pm 1.217$
Fe I	$-4.135 \pm 0.020$	$-4.110 \pm 0.008$	$7.137 \pm 0.626$	$-4.124 \pm 0.018$	$-4.111 \pm 0.006$	$7.094 \pm 0.632$
Fe II	$-4.117 \pm 0.060$	$-4.146 \pm 0.060$	$6.722 \pm 1.630$	$-4.121 \pm 0.057$	$-4.222 \pm 0.116$	$6.737 \pm 1.588$
Ni I	$-5.482 \pm 0.036$	$-5.469 \pm 0.033$	$7.596 \pm 1.064$	$-5.445 \pm 0.034$	$-5.434 \pm 0.036$	$7.539 \pm 1.066$
Ti I	$-6.815 \pm 0.058$	$-6.719 \pm 0.066$	$7.352 \pm 1.442$	$-6.728 \pm 0.059$	$-6.614 \pm 0.084$	$7.429 \pm 1.430$
Ti II	$-6.663 \pm 0.069$	$-7.037 \pm 0.152$	$7.407 \pm 1.453$	$-6.643 \pm 0.070$	$-7.040 \pm 0.141$	$7.444 \pm 1.460$

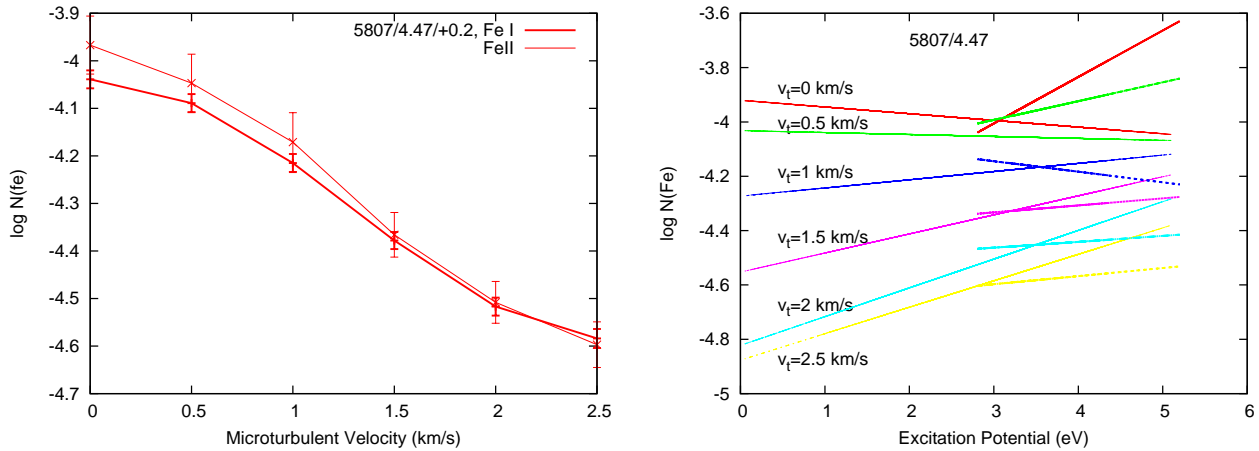


**Figure 3.** Left: abundances of iron determined from the fits on the synthetic spectra computed for the 5807/4.47/+0.2 model atmosphere to the observed Fe I and Fe II features in the observed spectrum of HD1835. Right: the dependence  $\log N(\text{Fe})$  vs.  $E''$  of Fe I and Fe II lines shown by thin and thick lines, respectively.

curacy of our  $T_{\text{eff}}$  determination for HD1835 is of the order  $\sim \pm 50\text{K}$ .

Using lines of different elements and ions we obtained the rotation velocity  $v \sin i = 7.2 \pm 0.5$  km/s. This value agrees with the determination from previous authors (see Jenkins et al. 2008 and references therein).

#### 4 HD10700

For the metal deficient star HD10700 we computed a small grid of model atmospheres of  $T_{\text{eff}} = 5133 - 5500$  K with a step of 50K and a  $\log g = 4.30 - 4.90$  with a step of 0.3. All models have a metallicity of  $[\text{Fe}/\text{H}] = -0.6$ . First of all, following Valenti & Fisher (2005) we adopted  $\log g = 4.59$  and obtained a good enough solution for two model atmospheres of  $T_{\text{eff}} = 5333$  and 5385 K. Both Fe I and Fe II solutions provide  $\log N(\text{Fe}) = -4.95 \pm 0.05$  for a rather low  $V_t = 0.5$  km/s, see (Fig. 4). A small dependence of  $\log N(\text{Fe}) = f(E'')$  is obtained for the Fe I lines, which cannot be removed by changes of  $T_{\text{eff}}$  and  $\log g$ . Again, the rotational velocity obtained from the fits of lines of different elements is in the range 2 - 2.7 km/s.

We then proceeded to investigate the dependence of our results on  $\log g$ . In general, the solution based on the

Fe I/Fe II ionisation equilibrium shows a systematic increase of  $T_{\text{eff}}$  in the case of model atmospheres of higher  $\log g$ , and vice versa, a decrease of  $\log g$  for the lower  $T_{\text{eff}}$ .

Nevertheless, we are able to obtain a good agreement in the Fe I/Fe II for cooler model atmospheres of lower  $\log g$  and hotter models of larger  $T_{\text{eff}}$  (see Fig. 5). Still using the  $\log N(\text{Fe})$  vs.  $E''$  proof we found that the hotter model atmospheres of higher gravities provide more reasonable results. Again, we obtain a self-consistent solution for the case of the rather low  $V_t$ , and, respectively, higher metallicity.

##### 4.0.1 Final remarks

The big advantage of our procedure is the possibility for independent proof of the measured results. First of all, our abundances and  $v \sin i$  show a rather weak dependence on the adopted parameters of the model atmosphere. We show that changes in the abundances are small (0.1 dex) if one is close to the appropriate temperature ( $\pm 100\text{K}$ ) and gravity ( $< 0.3$  dex) and thus our strategy is valid, at least for the solar-like stars of the solar neighborhood. Formal errors of our determination in most cases do not exceed 0.1 dex, a value that is good enough to determine abundances in the atmospheres of a large number of stars and perform statistical analyses on such samples.

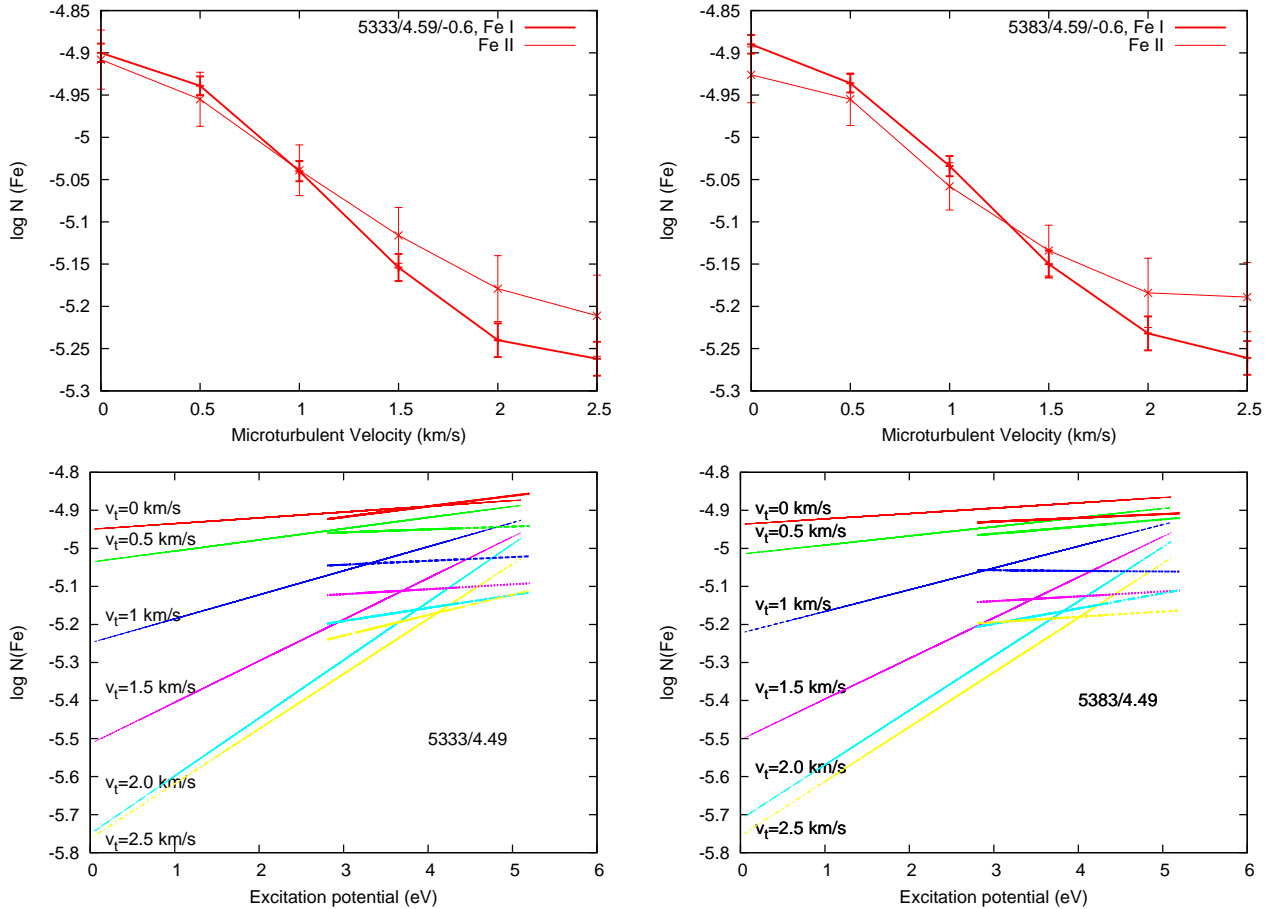


**Figure 4.** Top: abundances of iron determined from the fits of synthetic spectra computed for the 5333/4.49/-0.5 and 5383/4.90/-0.5 model atmospheres to the observed Fe I and Fe II features in the observed spectrum of HD10700. Bottom: the dependence  $\log N(\text{Fe})$  vs.  $E''$  of Fe I and Fe II lines is shown by thin and thick lines, respectively.

**Table 6.** Abundances in the atmosphere of HD10700

	5333/4.59/-0.6, $V_t = 0.5$ km/s			5383/4.49/-0.6, $V_t = 0.5$ km/s		
	Mean $\log [X/H]$	$\log [X/H]$ averaged	$v \sin i$	Mean $\log [X/H]$	$\log [X/H]$ averaged	$v \sin i$
Ca I	$-5.942 \pm 0.034$	$-5.958 \pm 0.131$	$2.250 \pm 0.678$	$-5.933 \pm 0.032$	$-5.943 \pm 0.108$	$2.167 \pm 0.653$
Cr I	$-6.837 \pm 0.024$	$-6.877 \pm 0.041$	$2.733 \pm 0.412$	$-6.814 \pm 0.024$	$-6.846 \pm 0.056$	$2.700 \pm 0.407$
Fe I	$-4.939 \pm 0.011$	$-4.911 \pm 0.005$	$2.622 \pm 0.230$	$-4.936 \pm 0.011$	$-4.910 \pm 0.005$	$2.580 \pm 0.226$
Fe II	$-4.955 \pm 0.032$	$-4.910 \pm 0.080$	$2.632 \pm 0.620$	$-4.955 \pm 0.031$	$-4.905 \pm 0.097$	$2.711 \pm 0.639$
Ni I	$-6.254 \pm 0.013$	$-6.257 \pm 0.061$	$2.000 \pm 0.283$	$-6.253 \pm 0.013$	$-6.250 \pm 0.051$	$2.000 \pm 0.283$
Ti I	$-7.298 \pm 0.035$	$-7.412 \pm 0.107$	$2.643 \pm 0.509$	$-7.271 \pm 0.034$	$-7.492 \pm 0.183$	$2.571 \pm 0.495$
Ti II	$-7.290 \pm 0.038$	$-7.239 \pm 0.105$	$2.500 \pm 0.521$	$-7.281 \pm 0.038$	$-7.257 \pm 0.104$	$2.521 \pm 0.526$

## 5 DISCUSSION

We have developed a numerical scheme which allows the determination of atomic abundances, microturbulent velocities and rotational velocities in stellar atmospheres in the framework of a self-consistent approach. Minimisation of the differences in the profiles of computed and observed lines allow us to carry out the determination of abundances of elements for neutral and ionic species separately. This allows us to provide an independent verification of the adopted ef-

fective temperatures, gravities and metallicities for the star in question.

We used the Sun as a template star to select the most appropriate lines of atoms and ions. Blending effects are accounted for directly, i.e., synthetic spectra are computed with the inclusion of all lines. This is important because even in the case of the solar spectrum we cannot fit to all lines without considering blends. To reduce possible numerical errors we account for only a part of each spectral feature



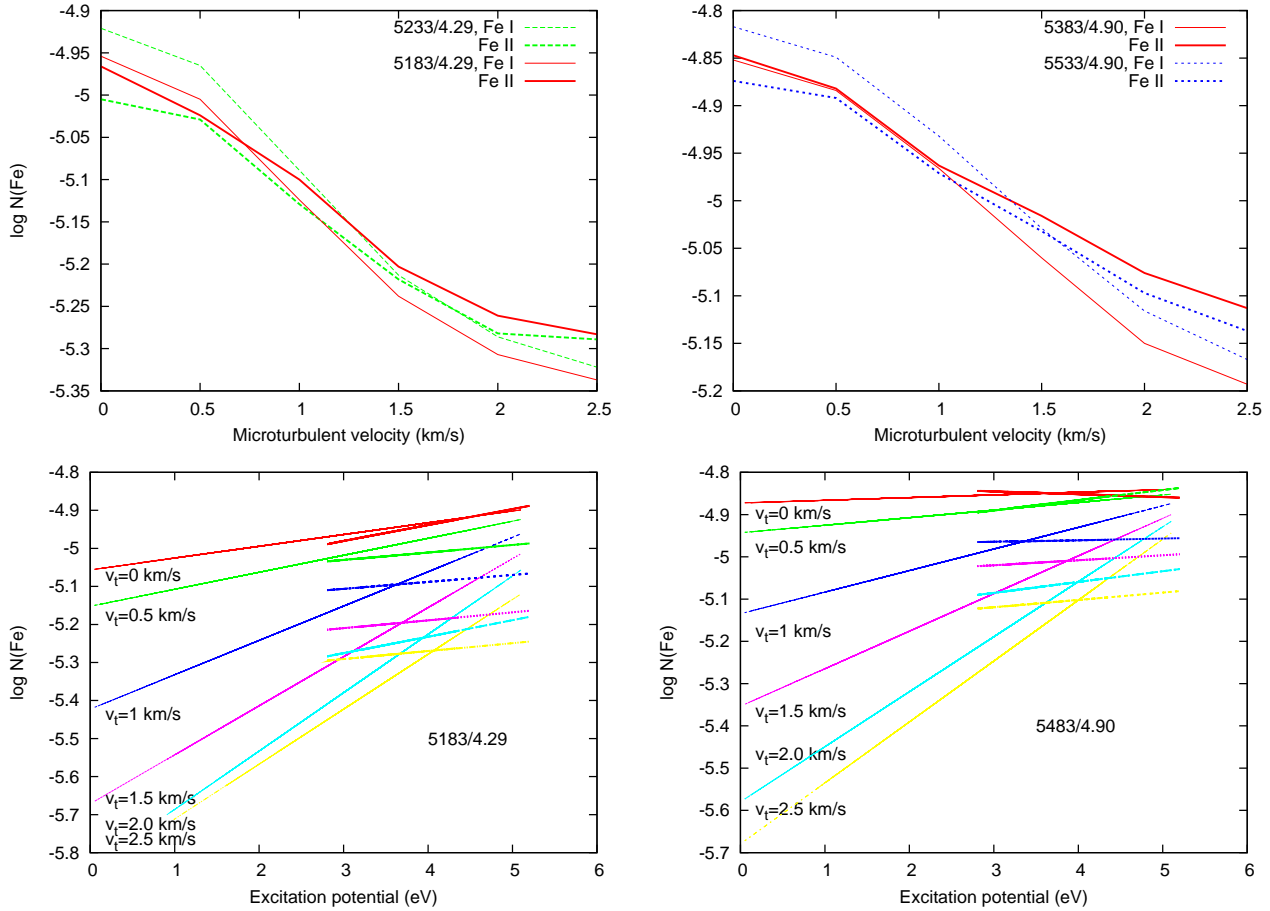


**Figure 5.** Top: abundances of iron determined from the fits of synthetic spectra computed for model atmospheres of different  $T_{\text{eff}}$  and  $\log g$  to the observed Fe I and Fe II features in the observed spectrum of HD10700. Bottom: the dependence  $\log N(\text{Fe})$  vs.  $E''$  of Fe I and Fe II lines is shown for the 5183/4.29 and 5483/4.90 model atmospheres by thin and thick lines, respectively.

**Table 7.** Abundances in atmospheres of our stars relative to the conventional solar abundances of GA89, i.e. Grevesse & Anders (1989) and GK89, i.e. Gurtovenko & Kostik (1989).

5777/4.44/0.0, $V_t = 0.5$ km/s		5807/4.47/+0.2, $V_t = 0.75$ km/s		5333/4.59/-0.6, $V_t = 0.5$ km/s		
	GK89	GA89	GK89	GA89	GK89	GA89
Ca I	0.068	$0.088 \pm 0.020$	0.398	$0.418 \pm 0.036$	-0.273	$-0.253 \pm 0.032$
Cr I	0.133	$0.063 \pm 0.021$	0.424	$0.354 \pm 0.034$	-0.374	$-0.444 \pm 0.024$
Fe I	0.005	$-0.025 \pm 0.007$	0.265	$0.235 \pm 0.020$	-0.536	$-0.566 \pm 0.011$
Fe II	-0.018	$-0.048 \pm 0.023$	0.283	$0.253 \pm 0.060$	-0.555	$-0.585 \pm 0.031$
Ni	0.075	$0.045 \pm 0.013$	0.338	$0.308 \pm 0.036$	-0.433	$-0.463 \pm 0.013$
TiI	-0.047	$0.023 \pm 0.019$	0.165	$0.235 \pm 0.058$	-0.291	$-0.221 \pm 0.034$
TiII	0.133	$0.203 \pm 0.037$	0.317	$0.387 \pm 0.069$	-0.301	$-0.231 \pm 0.038$

which shows a strong enough dependence on the adopted abundance. It is worth noting that the procedure of line selection from the solar spectrum was done within a narrow range of abundances. However, even in this case the fraction of blended lines can affect our results.

To derive abundances in the atmospheres of HD1835 and HD10700 we used the same list of spectral features governed by absorption lines determined from fits to the

solar spectrum. Our procedure works well enough for the case of metal rich stars (HD1835) and metal deficient stars (HD10700), for slow rotators (the Sun, HD10700), and intermediate fast rotators (HD1835). It is worth noting that for these 3 stars we have different levels of blending, and instrumental broadening.

Our approach uses the dependence of the minimisation factor  $S$  on three input parameters, i.e.  $\log N(\text{Fe})$ ,  $V_t$  and

$v \sin i$ . We show that our procedure allows us to find only one single solution across a range of reliable parameters. The metallicity of HD1835 is larger than the Sun, whereas HD10700 is found to be a metal deficient star. In all cases we obtained realistic results using our procedure. This provides some evidence to support the use of our procedure for studying the physical characteristics of solar-type stars.

As we know, previous authors have fit observed spectra to synthetic spectra by least squares methods to obtain stellar parameters (see Jones & Pavlenko 2002; Valenti & Fischer (2005); Jenkins et al. 2008 and references therein). Still our procedure determines abundances,  $V_t$ ,  $v \sin i$  in the framework of a self-consistent approach. Namely our abundances from the computed model atmospheres agree with the results of determinations using fits to the observed spectra. We used two independent proofs of the adopted model parameters: a) agreement of abundances of iron obtained from the fits to Fe I and Fe II lines, and b) the absence of any dependency of the iron abundance on excitation potential of Fe I and Fe II lines.

In the former papers, one or more parameters were fixed to simplify the procedure. Valenti & Fisher (2005) noted the degeneration of the procedure in respect to the  $V_t$  determination, and Jenkins et al. (2008) used a fixed value of  $V_t$  also. Furthermore:

- Our parameters in this paper were obtained by simple averaging across  $1\sigma$  error space. The final results we find agree well with literature values.
- We show that our solution is comparatively stable in respect to the small variations of the main input parameters:  $T_{\text{eff}}$ ,  $\log g$  and  $[\text{Fe}/\text{H}]$ . Still, we carried out our analysis in the framework of a self-consistent approach where the model atmosphere agree with the input parameters.

In our analyses we used Valenti & Fisher (2005)  $T_{\text{eff}}$  and  $\log g$  as a "zero approach" value. We extended the standard procedure by using the determination of the best agreement between the results, i.e.  $\log N(\text{Fe})$ ,  $\log g$ ,  $v \sin i$  and  $V_t$ , obtained from the fits to Fe I and Fe II lines in the framework of the self-consistent model. In general, our values of  $T_{\text{eff}}$  and  $\log g$  agree well with Valenti & Fisher values, but they were obtained with a smaller number of free parameters.

In our approach we determined  $[\text{Fe}/\text{H}]$ , microturbulent velocity and  $v \sin i$  from the best fits to the synthetic spectra, where these parameters are not free. Moreover, using abundances obtained by fits to lines of atoms and ions in the observed spectrum, we can, in principle, determine  $T_{\text{eff}}$  for these stars. Still, abundances are determined here from the fits to lines of atoms and ions separately, so that option is a part of our procedure for other stars. Abundances obtained for lines of Fe I and Fe II agree well for all three of the stars considered here. This confirms the effectiveness of our procedure. We note that, generally, the determination of  $\log g$  is difficult. Still most G-dwarfs lie on the main sequence, so their  $\log g$  should be approximately the same, around 4.5. Nevertheless, a more accurate  $\log g$  can be determined from the known parallaxes. Our results show some dependence on  $\log g$ . The fine analysis results of Tables 5 and 6 shows that we can determine all parameters from the best fits to Fe I and Fe II lines.

We plan to develop some methods to restrict possible  $\log g$  values using fits to strong lines presented in our spectra.

Wings of these lines are pressure broadened, so they are sensitive to  $\log g$  by definition. Also photometric criteria can be incorporated, such that we can iterate our solutions using each stars position on the HR-diagram.

We carry out our computations in the framework of the LTE approach. In principle, the effects of NLTE should be accounted for. However, the realisation of the NLTE concept is very difficult, even for the case Fe I and Fe II, (see Mashonkina et al. 2011 and references therein). We cannot expect large corrections of our results due to NLTE effects. Refined NLTE analysis by Mashonkina et al. shows that the average NLTE corrections amount to changes in the iron abundance of 0.01 - 0.1 dex. The value is within our formal error bars defined by our procedure and input data accuracy. The comparison of our iron abundances in the atmospheres of the Sun and HD10700 agree well with Mashonkina et al. (2011) to within  $\pm 0.1$  dex accuracy.

In general, the confidence of our solutions depend on the choice of input parameters. We confirm our solutions by comparing different parameters obtained from the fits of selected lines of Fe I, Fe II, and other elements to the observed spectrum. In fact, our results agree well with other recently published works for our three test cases.

Our procedure allows us to account for blending provided by other lines. In the most general case the efficiency of blending effects depend on resolution, metallicity and rotational velocity. Our experience shows that our procedure works for metal deficient and metal rich stars, stars with low and intermediate low (up to 20 km/s) rotational velocities, and over a range of  $T_{\text{eff}}$ 's. In the case of stars of low metallicities or fast rotators, the number of spectral lines which can be used is significantly reduced. That provides additional problems of the numerical analysis (see Ivanyuk et al. 2012). However, these problems are common for all known procedures.

We note two big advantages of our procedure: a) we use fits of theoretically computed profiles to the features in stellar observed spectra. This provides the possibility to determine the rotational velocities from the fits to all lines from our lists. b) Our procedure can be used for the abundance analysis of spectral data of the same quality obtained on high resolution spectrographs (e.g. FEROS, HARPS) for large numbers of stars.

## 6 ACKNOWLEDGEMENTS

The computations were carried out on the computer cluster of University of Hertfordshire. Work of YP and YL was partially supported by the "Cosmomicrophysics" program of the Academy of Sciences of Ukraine. YP, JHJ, DP, OI acknowledge funding by EU PF7 Marie Curie Initial Training Networks (ITN) ROPACS project (GA N 213646). JSJ acknowledges funding by Fondecyt through grant 3110004, along with partial support from Centro de Astrofisica FON-DAP 15010003, the GEMINI-CONICYT FUND and from joint committee ESO-Government of Chile grant. Authors thank Nick Malygin, Joana Gomes, Bogdan Kaminsky and our three anonymous referees for their helpful comments.

## REFERENCES

- Abia C., Rebolo, R., Beckman J. E., Crivellari L., 1988, *A&A*, 206, 100
- Arribas S., Crivellari L., 1989, *A&A*, 210, 211
- Barbuy B., Erdelyi-Mendes M., 1989, *A&A*, 214, 239
- Boesgaard A. M., Friel E. D., 1990, *ApJ*, 351, 467
- Boesgaard A. M., Budge K. G., 1988, *ApJ*, 332, 410
- Bruning D. H., 1984, *ApJ*, 281, 830
- Castro S., Porto de Mello G. F., da Silva L., 1999, *MNRAS*, 305, 693
- Cayrel R., Cayrel de Strobel G., Campbell B., 1985, *A&A*, 146, 249
- Cayrel de Strobel G., Knowles N., Hernandez G., Bentolila C., 1989, *A&A*, 94, 1
- Cayrel R., Cayrel de Strobel G., Campbell B., 1985, *A&A*, 146, 249
- Cenarro A. J. et al., 2007, *MNRAS*, 374, 664
- Francois P., 1986, *A&A*, 160, 264
- Ghezzi L., Cunha K., Smith V. V., de Araújo F. X., Schuler S. C., de la Reza R., 2010, *ApJ*, 720, 1290
- Glushneva I. N., Shenavrin V. I., Roshchina I. A., 2002, *A&AT*, 21, 317
- Gratton R. G., 1989, *A&A*, 208, 171
- Gurtovenko E. A., Kostik R. I., 1989, *Naukova D.*
- Gurtovenko E. A., Sheminova V. A., 1986, *Solar Phys.*, 106, 237.**
- Hearnshaw J. B., 1974, *A&A*, 34, 263
- Herbig G. H., 1965, *ApJ*, 141, 588
- Holweger H., Muller E. A., 1974, *Solar Phys.*, 39, 19
- Holweger H., Bard A., Kock M., Kock A., 1991, *A&A*, 249, 545
- Ivanyuk O. M., Pavlenko Ya. V., Jenkins, J. S., 2012, in preparation
- Israelian G., 2010, Evolution of Cosmic Objects through their Physical Activity. Viktor Ambartsumian's 100th anniversary Conf. Proc., Sep. 15-18, 2008, Yerevan, Byurakan, Armenia, Editors: Harutyunian H. A., Mickaelian A. M., Terzian Y., Yerevan, Gitutyun Publ. House, NAS RA, p. 318-337
- Jenkins J. S. et al., 2006, *MNRAS*, 372, 163
- Jenkins J. S., Jones H. R. A., Pavlenko Ya. V., Pinfield D. J., Barnes J. R., Lyubchik Yu., 2008, *A&A*, 485, 571
- Jenkins J. S., Ramsey L. W., Jones H. R. A., Pavlenko Ya. V., Gallardo J., Barnes J. R., Pinfield D. J., 2009a, *ApJ*, 704, 975
- Jenkins J. S. et al., 2009b, *MNRAS*, 398, 911
- Jenkins J. S., Murgas F., Rojo P., Jones H. R. A., Day-Jones A. C., Jones M. I., Clarke J. R. A., Ruiz M. T., Pinfield D. J., 2011, *A&A*, 531, 8
- Kupka F., Piskunov N., Ryabchikova T. A., Stempels H. C., Weiss W. W., 1999, *A&AS*, 138, 119
- Kurucz R. L., Furenlid I., Brault J., Testerman L., 1984, *National Solar Observatory Atlas*, 198
- Kurucz R. L., 1993, *ASP Conf. Ser.*, 44, 87
- Lopez-Santiago J., Montes D., Galvez-Ortiz M. C., Crespo-Chacon I., Martínez-Arnáiz R. M., Fernandez-Figueroa M. J., de Castro E., Cornide M., 2010, *A&A*, 514, 97
- Mallik S. V., 1998, *A&A*, 338, 623
- Martínez-Arnáiz R., Maldonado J., Montes D., Eiroa C., Montesinos B., 2010, *A&A*, 520, 79.
- Mashonkina L., Gehren T., Shi J.-R., Korn A.J., Grupp F., 2011, *A&A*, A87
- Neves V., Santos N. C., Sousa S. G., Correia A. C. M., Israelian G., 2009, *A&A*, 497, 563
- Pagel B. E. J., 1964, *Royal Observatory Bulletins*, 87, 227
- Pagel B. E. J., 1963, *JQSRT*, 3, 139
- Pasquini L., Liu Q., Pallavicini R., 1994, *A&A*, 287, 191
- Pavlenko Ya. V., 1997, *A&AS*, 253, 43
- Pavlenko Ya. V., 2003, *Astron. Rept.*, 47, 59
- Rebolo R., Beckman J. E., Crivellari L., Castelli F., Foing B., 1986, *A&A*, 166, 195
- Santos N. C. et al., 2011, *A&A*, 526A, 112
- Sheminova V. A., Gadun A. S., 2010, **Fourier analysis of Fe I lines in the spectra of the Sun,  $\alpha$  Centauri A, Procyon, Arcturus, and Canopus** (<http://arxiv.org/abs/1004.3286>).
- Soubiran C., Bienayma O., Mishenina T. V., Kovtyukh V. V., 2008, *A&A*, 480, 91
- Sousa S. G. et al., 2008, *A&A*, 487, 373
- Sousa S. G., Santos N. C., Israelian G., Mayor M., Udry S., 2011, *A&A*, 533A, 141
- Snedden C., Johnson H. R., Krupp B. M., 1976, *ApJ*, 204, 218
- Steenbock W., 1983, *A&A*, 126, 325
- Tabernerero H. M.; Montes D.; Gonzalez Hernandez J. I., 2011, <http://cdsads.u-strasbg.fr/abs/2011hsa6.conf.551>.
- Takeda Y., Honda S., Kawanomoto S., Ando H., Sakurai T., 2010, *A&A*, 515, 93
- Teixeira T. C. et al., 2009, *A&A*, 494, 237
- Tomkin J., Lambert D. L., 1999, *ApJ*, 523, 234
- Valenti J., Fischer D., 2005, *ApJS*, 159, 141
- Willie S., Peter F., Sallie B., 1999, *ApJ*, 510L, 135
- Unsold A., 1956, *Physics der Sternatmosphären*. American Institute of Physics, NY